https://doi.org/10.1016/j.ijrmhm.2019.105048

Effects of binder concentration on the nanometric surface characteristics of WC-Co materials in ultra-precision grinding

Quanli Zhang[1, 2*], Nan Guo[1], Yan Chen[1,2] and Suet To[3]

[1] Jiangsu Key Laboratory of Precision and Micro-Manufacturing Technology, Nanjing University of Aeronautics and Astronautics, Nanjing, 210016, China

[2] College of Mechanical and Electrical Engineering, Nanjing University of Aeronautics and Astronautics, Nanjing, 210016, China

[3] State Key Laboratory of Ultra-precision Machining Technology, The Hong Kong Polytechnic University, Hong Kong

*Corresponding Author / E-mail: zhangql@nuaa.edu.cn, TEL: +86-25 84892901, FAX: +86-25 84892901

Abstract

The influence of the binder concentration on the nanometric surface characteristics of WC/Co in ultra-precision grinding is investigated in the present work. The results firstly show that the surface finish of the ground WC/Co changed with increasing Co content, and the machined surfaces were covered by many micro-pits and surface burs induced by the plastic deformation and the prior removal of Co binder, which also led to the micro-chipping of the WC grains near the boundaries for the lack of support by Co. Many finer scratching grooves in the feed marks appeared, but the periodic grinding grooves caused by the feed of the diamond wheel became unclear with increasing Co content and the vibration induced marks on the machined surface turned to be primary, the spatial frequency of which is identified to be around 130 1/mm by the Fast Fourier transform. In addition, for the isotropic of the statistical size of the WC grains and the thickness of Co binder along each direction, a circular symmetry shape of the spatial frequency forms and the radius increases with increasing Co content.

Keywords: WC/Co; Binder concentration; Nanometric surface characteristics; Ultra-precision grinding

1. Introduction

For the excellent mechanical properties at high temperature and severe environments, cemented carbides have been widely applied as the cutting tools, the glass molding dies and the heat resistant part of the aero-engine, etc.. However, the great brittleness of the bulk materials limits its wider application, and an appropriate amount of metal binder (Co, Ni, etc.) is added to improve the ductility of the bulk materials based on the requirement of a specific application. It is certain that the mechanical properties and the damage mechanics of the bulk WC/Co materials under mechanical loading change with different binder content, and the micro-cracking toughening mechanism proposed by Sigl et al applies well to WC/Co [1], where a great amount of phase boundaries existed in the bulk materials, especially for the nano-grain sized WC [2, 3]. In addition, the addition of the metal binder also contributes to the improvement of the machinability of the bulk materials in the grinding process. A few studies have been performed to reveal the effects of the WC grain size and the binder addition on the surface damage mechanism of WC/Co under the mechanical loading, and the nanometric surface characteristics of the ground WC/Co have been widely investigated, where a severely plastic deformation layer was induced during the machining process [4]. For examples, Hegeman et al [4] presented that the surface roughness of the ground surface was dependent on the grain size, and it was characterized by a deformed layer and the prismatic slip and cracks in the WC grain were clearly found. Nano-indentation and scratching test of the cemented carbides of different grain size by Duszová et al, Ndlovu et al, and Sun et al [5-7], and they reported that the cobalt extrusion, grain fracture and deformation appeared during the scratch, depending on both of the WC grain size and the Co content. The surface damage mechanics of WC/Co under the mechanic loading were always found to be plastic scratching grooves, cobalt binder extrusion and phase boundaries fracture [8-10]. Considering the complex environment in the grinding zone, chemical reaction of the surface material occurred under the high temperature and high pressure [11], that is, the oxidation od WC and Co binder. As has been mentioned above, the interfaces between the WC grains and the Co binder play a dominant role on the mechanical properties of WC/Co bulk materials, and the addition of the Co binder also affects the wear mechanism [10]. For the varied hardness of WC and Co, the material removal rate also differed under the abrasive machining process by the diamond wheels, which resulted in the decrease of the bonding strength of the WC grains and the formation of the surface

reliefs, as well as the micro-pits, on the ground surface [2]. In addition, the high pressure exerted by the abrasive grits led to the phase transformation of the fcc-hcp Co [7], and the binder deformation might transfer from the phase transformation to slip plus twinning with increasing Co binder [12]. Actually, the mean free path of WC grains (λ) in the bulk materials changed with the increase of the Co [13], which could bear great effect on the formation and propagation of the surface cracking and plastic deformation [14]. The inter- and trans-granular carbide fracture, as well as the fracture at the carbide grain-binder interfaces, were proposed as the main failure mechanism by Sigl et al. [15]. However, the complex loading condition in the grinding zone always results in some unexpected experimental results, and the subsurface microstructure evolution under the repeated grinding process still need further exploration to improve the surface quality of the ground surface. Therefore, it is beneficial to get a further understanding of the influence of the binder concentration on the surface damage and the generation mechanism of WC/Co.

In the present work, the effects of the binder concentration on the nanometric surface characteristics of WC/Co under ultra-precision grinding are investigated, where the surface fracturing, the surface burs and the micro-pits formation mechanism are explored. Besides, the 2D FFT (Fast Fourier transform) analysis of the machined surface are also performed to get a deep insight into the nanometric surface characteristics. The obtained research results can provide theoretical and technical supports for the ultra-precision grinding of the cemented carbides.

2. Experiments and materials

Commercially available WC/Co bulk materials with different Co content (Binderless 0 wt. %, 8 wt. %, 15 wt. % and 20 wt. %) were applied as the workpiece materials, and the ultra-precision grinding experiments were conducted on an ultra-precision machine tool (Moore Nanotech 450UPL. USA). The photograph of the grinding setup is shown in Fig. 1. The 1500# diamond wheel used was resin bonded and the diameter was 20 mm with a carbide mandrel (Diagrind, Inc., USA). Before the grinding process, dressing of the wheel was performed by a rotating Al_2O_3 stick and a 60 ° sharp edge was obtained. The detail information of the dressing parameters can be found in the previous work [16]. In addition, Vickers indentations of the polished surface with the surface roughness (*Sa*) lower than 10 nm were also undertaken to investigate the damage behavior of WC/Co under the varying loading/unloading conditions.

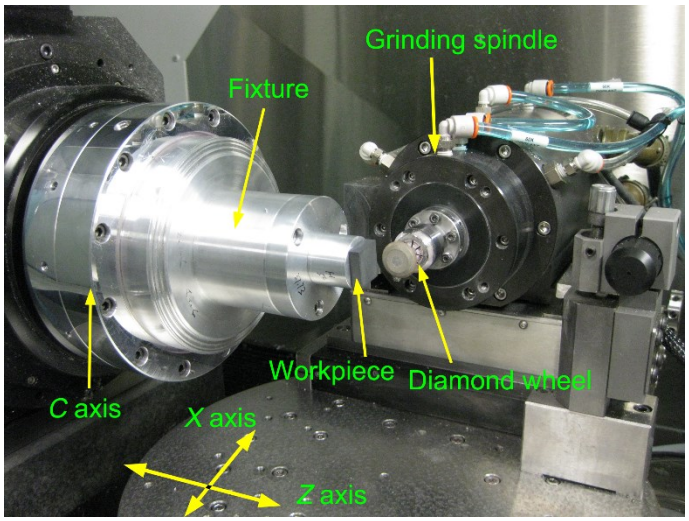

Fig. 1. Photograph of the ultra-precision grinding machine

The 3D surface topography of the ground WC/Co was measured by a white light interferometer (WLI, Nexview 3D profiler, ZygoLamda) and an atomic force microscope (AFM, Park's XE-70), where the surface roughness parameters *Sa*, *Sq* and *St* were obtained, which refers to the arithmetical mean height calculated over the entire measured array, the root mean square height calculated over the entire measured array and the maximum peak-to-valley difference calculated over the entire measured array according to the standardization and formalization of the analysis of 3D surface texture (ISO 25178-2:2012), respectively. The surface morphology of the ground WC/Co and the indentation imprints was examined by a scanning electron microscope (SEM, Hitachi TM3000).

3. Results and discussions

The surface topography of the ground WC carbides is shown in Fig. 2. It can be seen that the machined surfaces are covered by obvious grinding grooves, especially for the binderless WC and the WC/8Co. With increasing Co content, many micro-pits appear and the average size grows, which distribute randomly on the ground surface. Correspondingly, the surface roughness (*Sa*, *Sq* and *St*) at the same radial distance for the machined surface increases with increasing Co binder content slightly.

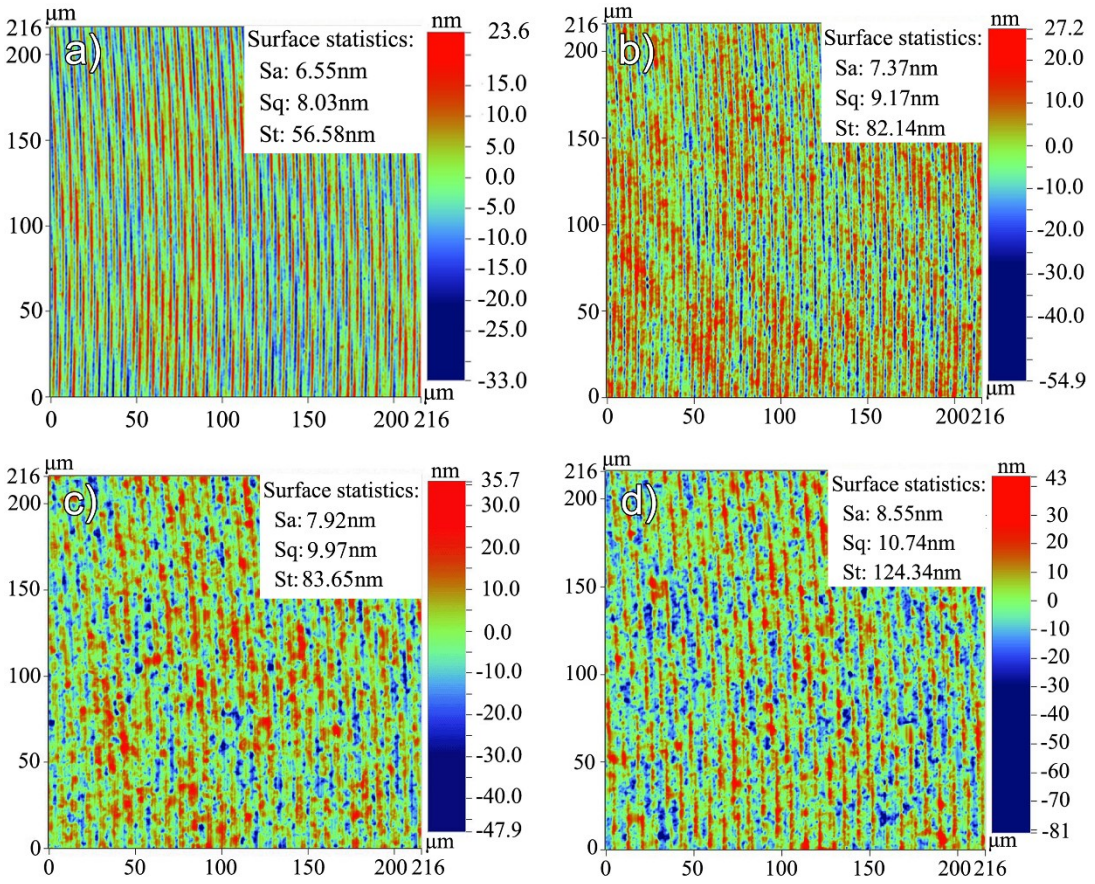

Fig. 2. Surface topography of the machined cemented carbides: (a) Binderless WC; (b) WC/8Co; (c) WC/15Co; (d) WC/20Co

The surface morphology of the ground WC carbides is shown in Fig. 3. For the binderless WC, the machined surface is characterized by the plastic grinding grooves (indicated by the green arrows in Fig. 3) which are mainly caused by the feed of the diamond grinding wheel along the radial direction. In addition, the depth of the finer grooves induced by the diamond grits varies due to the stochastic distribution of the protrusion height and the diameter of the grits. For the particular processing technology, the grain boundaries for binderless WC are not exposed after grinding. With the addition of the Co binder, the effects of the grain boundaries become more obvious, except for the grinding grooves remained on the machined surface. Specifically, the grain boundary fracturing (indicated by the red arrows in Fig. 3) appeared under the scratching effects of the diamond grits, and the prior removal of Co led to the generation of the surface reliefs for the different hardness between the WC grains and the Co binder. Therefore, the lack of support for the edge of the WC grains resulted in the micro-fracturing, which had also been proved by the nano-indentation test and the diamond scratching test in the previous study[11, 17]. The higher

content of the Co binder, the more obvious of the grain boundary fracturing, as shown in Fig. 3(c) and Fig. 3(d).

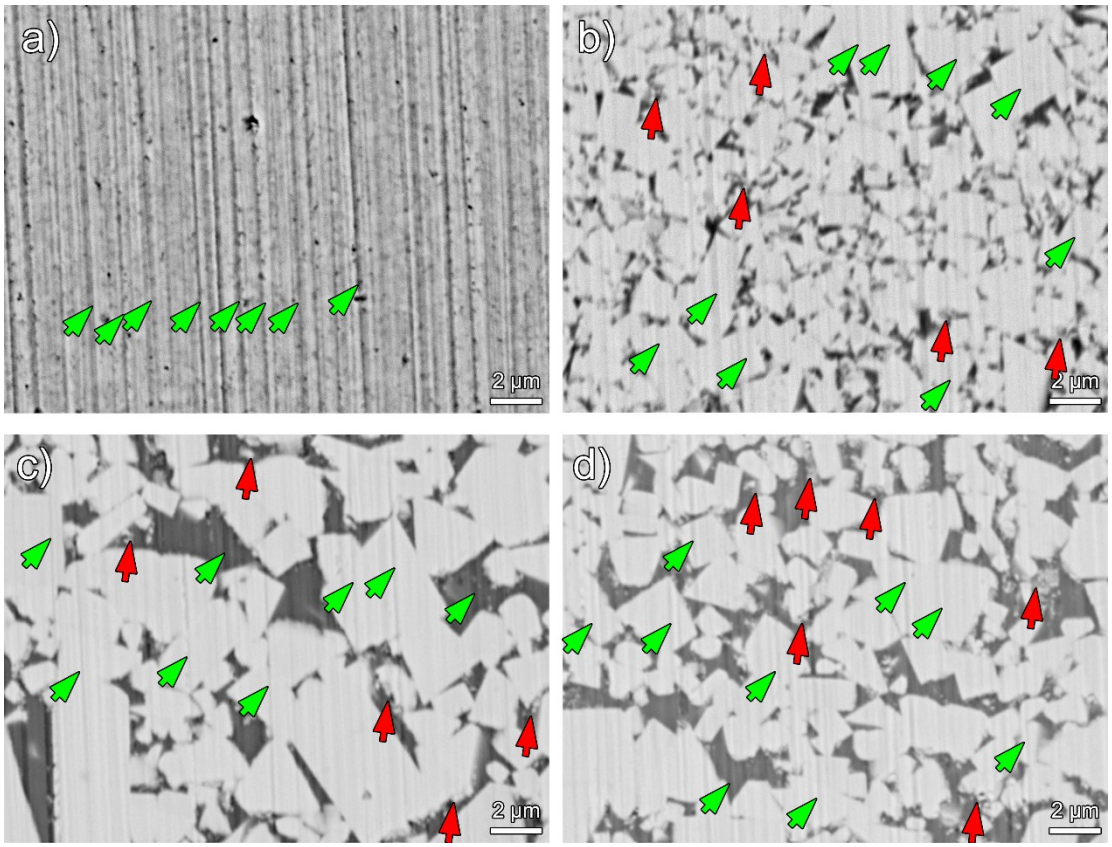

Fig. 3. SEM images of the machined cemented carbides: (a) Binderless WC; (b) WC/8Co; (c) WC/15Co; (d) WC/20Co, where the green arrows represent the grinding grooves and the red arrows indicate the grain boundary fracture

From the nanometric surface topography of the machined cemented carbides shown in Fig. 4, it can be seen that some bulges (indicated by the magenta arrows) formed on the machined surfaces of WC/15Co and WC/20Co, and they mainly distributed at the phase boundaries. Under the exerted pressure of the diamond grits, the extrusion of Co and the fracturing WC grains should account for the appearance of the bulges on WC/15Co and WC/20Co [9]. In comparison, the machined WC/8Co surface appears much more clear, as shown in Fig. 4(a) and Fig. 4(b), where only some micro-pits were generated. Moreover, the machined surfaces are covered by many irregular finer scratching grooves of different depth due to the random distribution and the stochastic protrusion heights of the diamond grits in the resin bonded wheel [18].

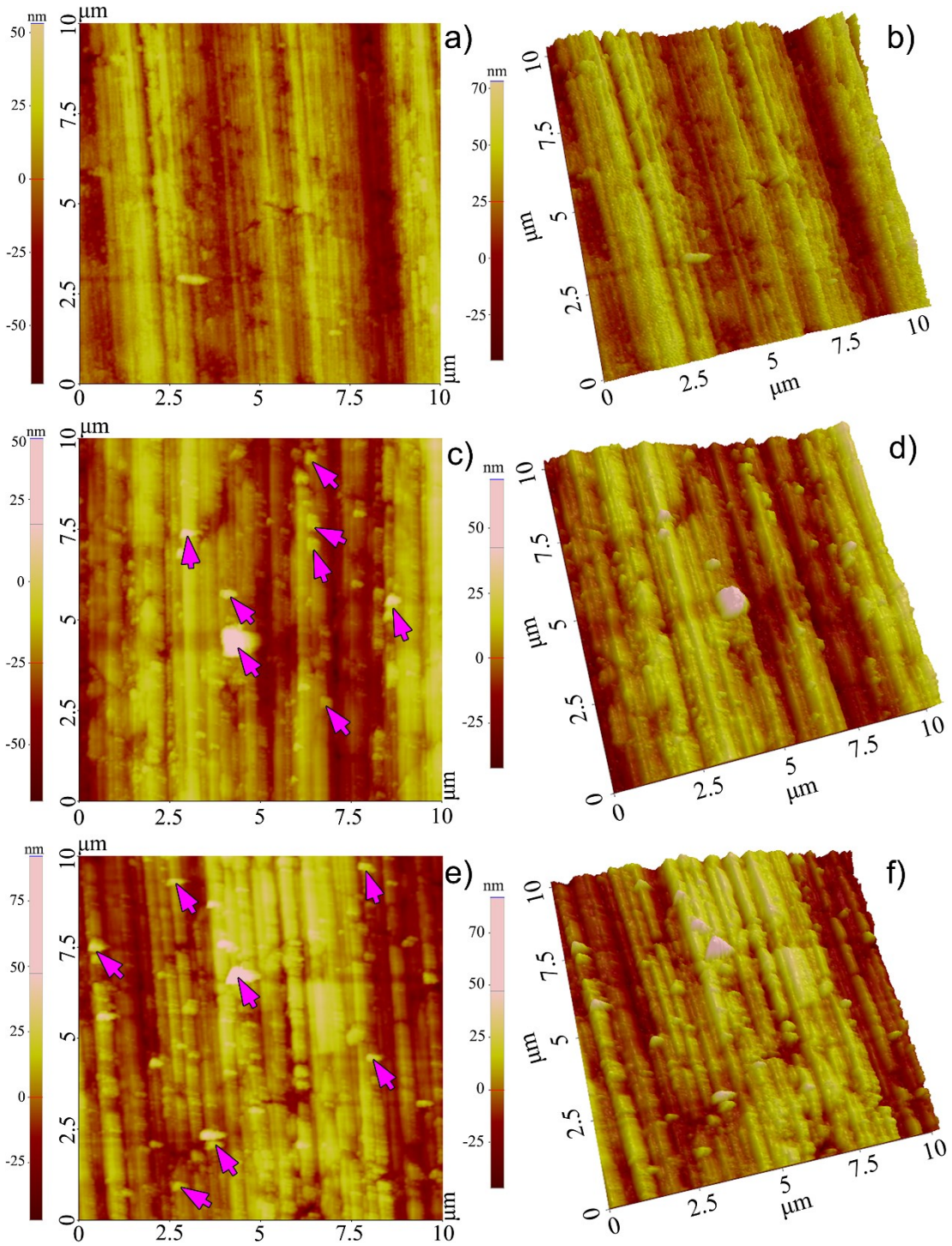

Fig. 4. Surface topography of the machined cemented carbides: (a) WC/8Co; (b) WC/15Co; (c) WC/20Co, where the magenta arrows indicate the surface bulges

The cross-sectional profiles of the machined surface indicate that the amplitude of the surface waviness grows with increasing Co binder and the conformity also becomes weak, as shown in Fig. 5, which even leads to the disappearance of scratching grooves caused by the feed of the diamond wheel. Meantime, the vibration marks on the machined surface also turn to be irregular

due to the formation of the larger micro-pits.

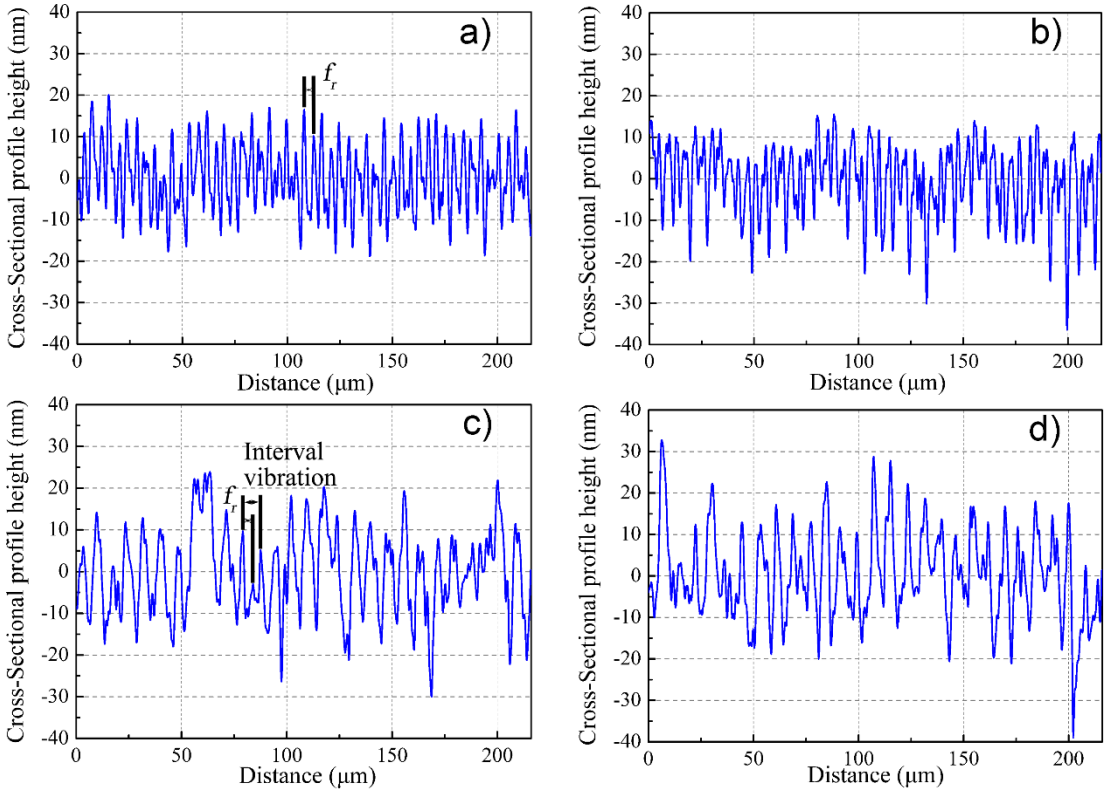

Fig. 5. Cross-sectional profiles of the machined WC/Co carbides：(a) Binderless WC; (b) WC/8Co; (c) WC/15Co; (d) WC/20Co

The compared results of the Vickers hardness indentation tests at 5 kg show us more information on the damage mechanics of the grain boundaries, as shown in Fig. 6. The binderless WC experienced an obvious cracking process during the indentation process, with the length of the radial cracks to be around 200 μm, indicating the weaker toughness. Interestingly, the layered cracking occurred in the indentation imprints, as shown in Fig. 6(b), which might be caused by the progressive loading condition. For the WC/15Co material, no radial cracks were induced under the same loading conditions, but the size of the imprints increases, indicating the improved toughness and the lower hardness of the bulk WC/Co materials after adding Co binder. An enlarged area at the bottom of the imprint, as shown in Fig. 6(d), indicates that the transgranular cracking is aroused to cooperate the plastic deformation. In addition, the slipping bands along the loading direction in the WC grains can be clearly found along with the micro-cracking, where the severe plastic deformation of the WC grains contributes to the boundaries fracture [19].

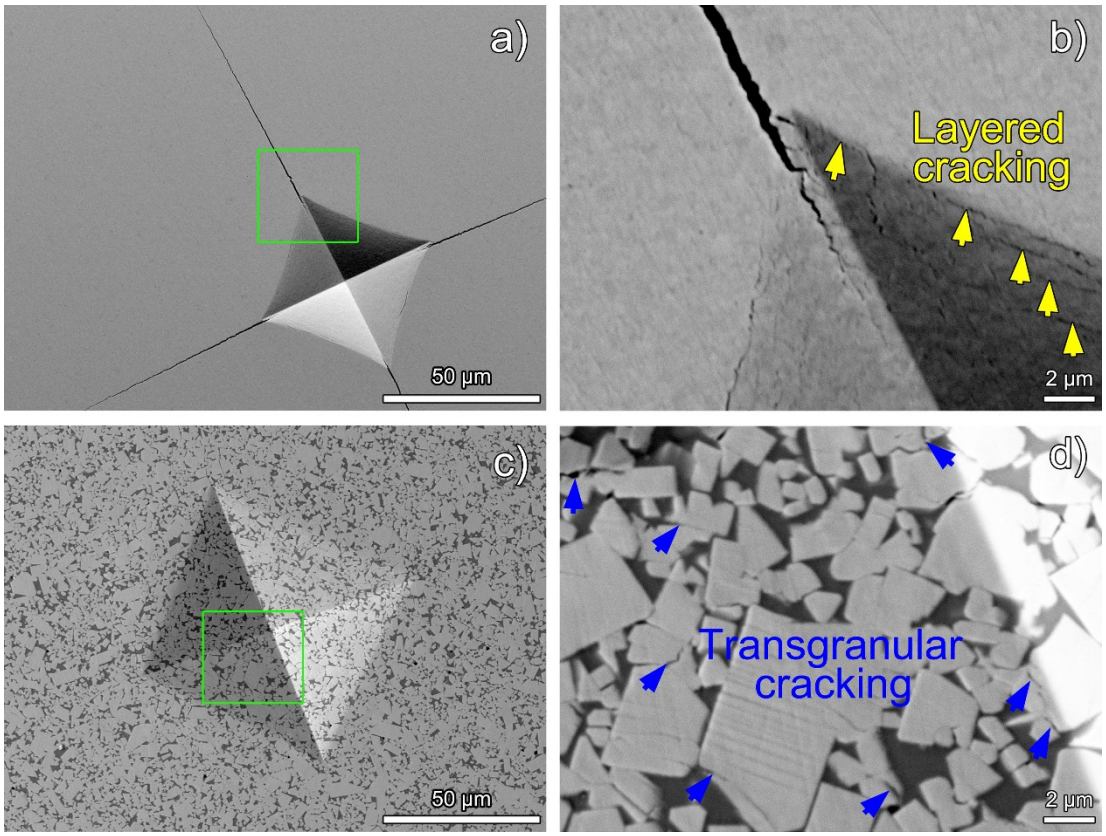

Fig. 6. SEM images of the Vickers indentation imprints for: (a) and (b) Binderless WC; (c) and (d) WC/15Co, where the yellow arrows indicate the layered cracking and the blue arrows indicate the transgranular cracking

For the varying hardness between the Co binder and the WC grains, the material removal rate also differ even under the same grinding process, and the prior removal of the Co binder contributes to the formation of the surface reliefs and the unsupported WC grains edge. The extrusion of Co binder through the neighboring WC grains loaded by the diamond grains became obvious with higher Co binder content, as shown in Fig. 3. These all mean that the increasing Co binder content in the bulk materials results in a declined surface quality of the cemented carbides, as shown in Fig. 7. Except for the singular surface statistics of the center area caused by the diamond wheel wear and the tool installation error [20, 21], the surface roughness (*Sa* and *Sq*) of the machined WC/Co carbides grows with increasing Co content. However, the value for *St* at different radial distance on the machined surface changed in a certain way with increasing radial distance, which might be attributed to the radial vibration between the wheel and the workpiece [22, 23].

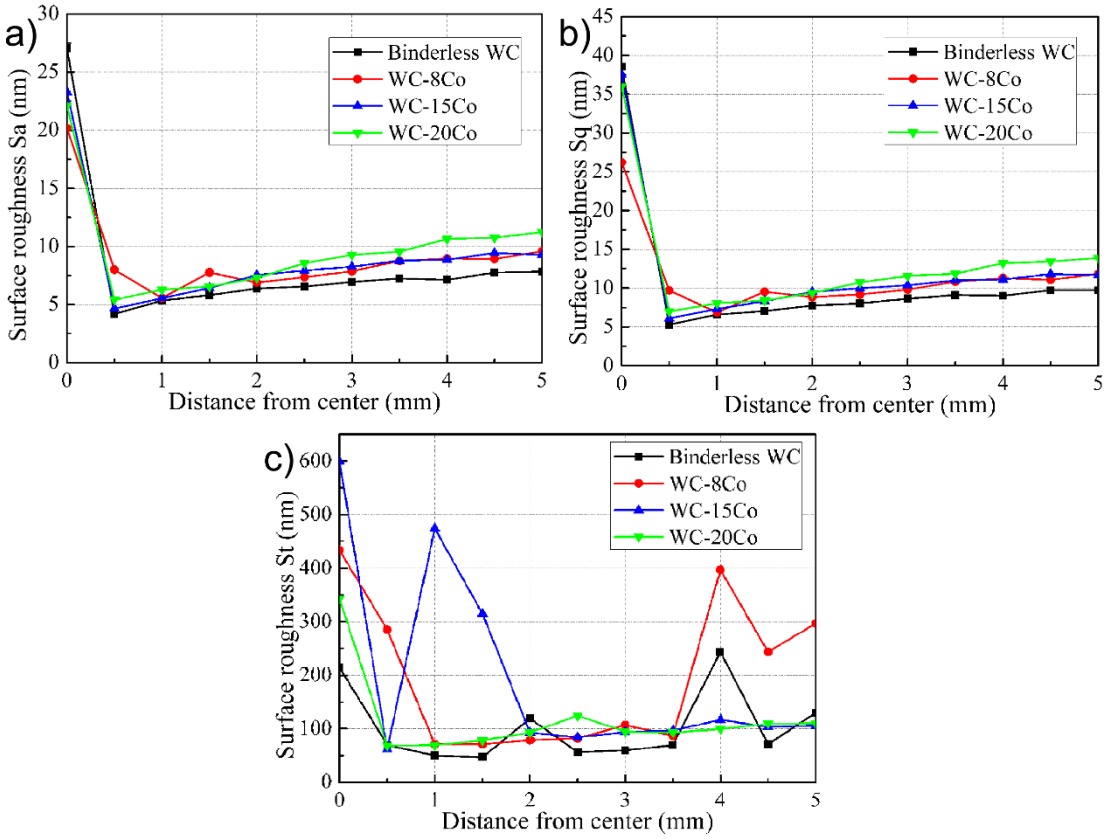

Fig. 7. Surface roughness against the radial distance from center: (a) *Sa*, (b) *Sq*, (c) *St*

To get a further insight into the surface characteristics, the obtained surface datasets are treated by a Fast Fourier Transform (FFT) program based on the Matlab software. The obtained 2D spatial frequency of the machined surface is shown in Fig. 8. It can be easily found that the typical spatial frequency obtained corresponds to the tool feed frequency which can be achieved by the following equations [24],

$$f_{spatial} = \frac{1}{d_{pp} \times 10^{-3}} \tag{1}$$

$$\nu_{F1,nf} = \frac{n_f + 1}{f_r}, \text{ for } n_f = 0, 1, 2, \ldots \tag{2}$$

Where $f_{spatial}$ is the spatial frequency corresponding to the measured waviness peak values d_{pp}, $\upsilon_{F1,nf}$ is the tool feed frequency, and f_r is the feed rate per revolution. The feed rate per workpiece rotation is 4.17 μm，and the corresponding spatial frequency is theoretically calculated to be 239.8 1/mm along the feed direction. As shown in Fig. 8(a), the tool feed frequency on the machined cemented carbides surface at around 236.6 1/mm can be clearly identified for all of them, but the peak intensity drops with the increase of the Co binder content. Instead, the spatial frequency at

around 130 1/mm appears and the intensity gradually turns to be dominant with a higher Co content. This is attributed to the fact that the higher Co content results in the formation of many micro-pits and the random boundaries of the WC grains which lead to the weakened feed marks of the diamond wheel on the machined surface. As shown in Fig. 2, compared with the binderless WC, the feed marks on the machined WC/15Co and WC/20Co even disappeared, with the regular vibration marks remained clear. Actually, it is the related tool-workpiece vibration that contributes to the appearance of 130 1/mm that is the peak-to-valley distance of about 7.65 μm, as shown in Fig. 2 and Fig. 5. In addition, the spatial frequency at around 51 1/mm, 366.5 1/mm and some small peaks are attributed to the phase sift of the relative vibration between the diamond wheel and the workpiece [22]. The varying protruding height and the micro-chipping of the diamond grits resulted in the generation of much finer grooves [20].

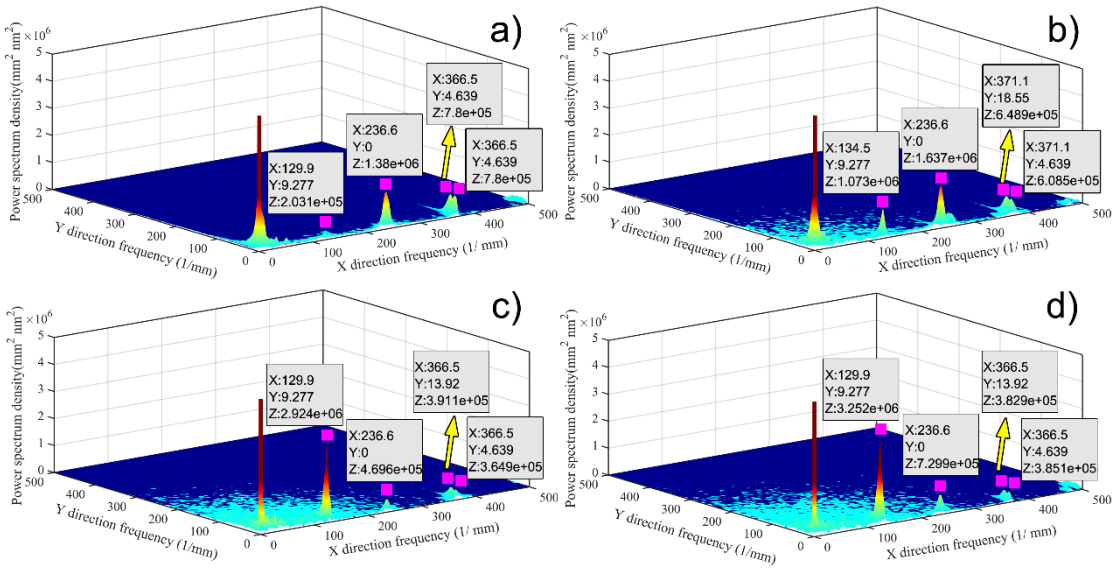

Fig. 8. Power spectra densities of the surface profiles for: (a) Binderless WC; (b) WC/8Co; (c) WC/15Co; (d) WC/20Co

As shown in Fig. 9, it can be seen from the polished WC/Co materials that no obvious defects exist in the original bulk material. The size and the posture of the WC grains vary， where the dark areas are Co binder and the gray areas are WC grains. Besides, the thickness of the Co binder between the WC particles, that is the mean free path, also differs [25]. Even in the polishing process, the extra removal of Co was identified, resulting in a higher residual height of the WC grains [26], where the easier removal of Co results in the formation of the surface reliefs during the surface polishing process, as shown in Fig. 9(c) and Fig. 9(d). This is also found to appear for

the grinding process of WC/Co [2]. Therefore, for the isotropic of the statistical size of WC grains, the thickness of Co binder along each direction and the generated surface reliefs, a circular symmetry shape of the spatial frequency forms and the radius grows with increasing Co content.

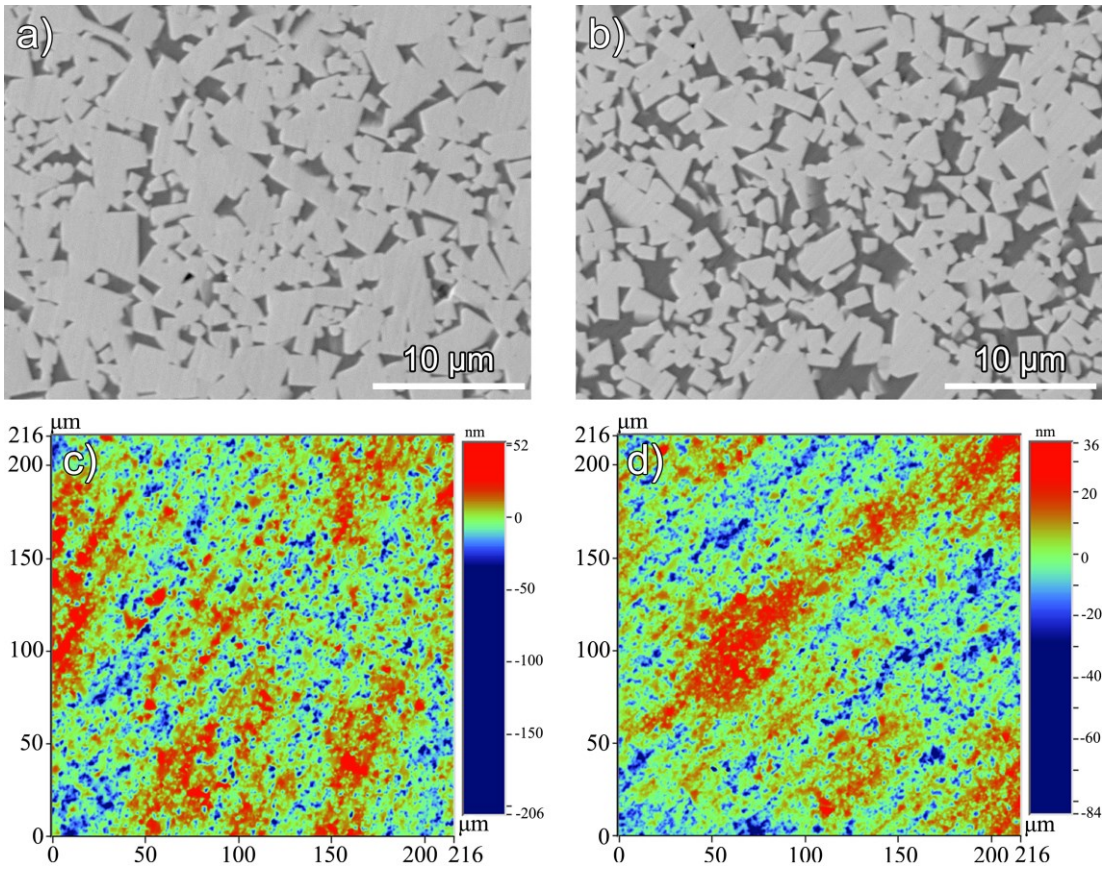

Fig. 9. SEM images and 3D surface topography of the polished WC/15Co and WC/20Co carbides: (a) and (c) WC/15Co, (b) and (d) WC/20Co

4. Conclusions

The nanometric surface characteristics of WC/Co with different binder concentration (0%, 8%, 15% and 20%)in ultra-precision grinding are explored in the present work. Based on the analysis of the 3D surface topography, the surface morphology, the cross-sectional profile and the 2D FFT results of the surface datasets, the following conclusions can be achieved,

(1) With increasing Co concentration, the nanometric surface finish of the WC/Co obtained in ultra-precision grinding dropped, where the surface burs were easily induced under the extrusion of the Co binder;

(2) Even though the addition of Co binder contributed to the improvement of the toughness, the prior removal of Co binder led to the generation of many micro-pits and the edge chipping of the WC grains for the lack of the support;

(3) Many finer scratching grooves in the feed marks appeared, but the regular grinding grooves caused by the feed of the diamond wheel became unclear with increasing Co content and the vibration induced marks on the machined surface turned to be primary, the spatial frequency of which was identified to be around 130 1/mm by the Fast Fourier transform.

Acknowledgements

The work was supported by the National Natural Science Foundation of China (NSFC) (Project No.:51805257), the China Postdoctoral Science Foundation funded project (Project No.:2019TQ0146) and the Jiangsu Key Laboratory of Precision and Micro-Manufacturing Technology. In addition, the authors would like to show great thanks to Mr. Tai Wa Chung for his kind help in the experiments.

References

[1] L.S. Sigl, Microcrack toughening in brittle materials containing weak and strong interfaces, Acta Materialia 44 (1996) 3599-3609.

[2] Q. Zhang, S. To, Q. Zhao, B. Guo, M. Wu, Effects of binder addition on the surface generation mechanism of WC/Co during high spindle speed grinding (HSSG), Int. J. Refract. Met. Hard Mater. 59 (2016) 32-39.

[3] Z.Z. Fang, X. Wang, T. Ryu, K.S. Hwang, H.Y. Sohn, Synthesis, sintering, and mechanical properties of nanocrystalline cemented tungsten carbide-A review, Int. J. Refract. Met. Hard Mater. 27 (2009) 288-299.

[4] J.B.J.W. Hegeman, J.T.M. De Hosson, G. de With, Grinding of WC-Co hardmetals, Wear 248 (2001) 187-196.

[5] S. Ndlovu, K. Durst, M. Göken, Investigation of the sliding contact properties of WC-Co hard metals using nanoscratch testing, Wear 263 (2007) 1602-1609.

[6] H.Q. Sun, R. Irwan, H. Huang, G.W. Stachowiak, Surface characteristics and removal mechanism of cemented tungsten carbides in nanoscratching, Wear 268 (2010) 1400-1408.

[7] A. Duszová, P. Hvizdoš, F. Lofaj, A. Major, J. Dusza, J. Morgiel, Indentation fatigue of WC-Co cemented carbides, Int. J. Refract. Met. Hard Mater. 41 (2013) 229-235.

[8] M.G. Gee, L. Nimishakavi, Model single point abrasion experiments on WC/Co hardmetals, Int. J. Refract. Met. Hard Mater. 29 (2011) 1-9.

[9] M. Gee, K. Mingard, J. Nunn, B. Roebuck, A. Gant, In situ scratch testing and abrasion simulation of WC/Co, Int. J. Refract. Met. Hard Mater. 62 (2017) 192-201.

[10] A.J. Gant, M.G. Gee, D.D. Gohil, H.G. Jones, L.P. Orkney, Use of FIB/SEM to assess the tribo-corrosion of WC/Co hardmetals in model single point abrasion experiments, Tribol. Int. 68 (2013) 56-66.

[11] Q. Zhang, Z. Zhang, Y. Fu, Surface damage mechanics of WC/Co composites investigated by indentation and diamond scratch, Mater. Res. Express 6 (2019) 16514.

[12] C.H. Vasel, A.D. Krawitz, E.F. Drake, E.A. Kenik, Binder deformation in WC-(Co, Ni) cemented carbide composites, Metall. Mater. A 16 (1985) 2309-2317.

[13] V. Kumar, Z.Z. Fang, S.I. Wright, M.M. Nowell, An analysis of grain boundaries and grain growth in cemented tungsten carbide using orientation imaging microscopy, Metall. Mater. Trans. A 37 (2006) 599-607.

[14] S. Paul, A. Ghosh, Grinding of WC-Co cermets using hexagonal boron nitride nano-aerosol, Int. J. Refract. Met. Hard Mater. 78 (2019) 264-272.

[15] L.S. Sigl, H.E. Exner, Experimental study of the mechanics of fracture in WC-Co alloys, Metall. Mater. A 18 (1987) 1299-1308.

[16] Q. Zhang, Q. Zhao, S. To, B. Guo, Z. Rao, Precision machining of 'water-drop' surface by single point diamond grinding, Precis. Eng. 51 (2018) 190-197.

[17] M. Bľanda, A. Duszová, T. Csanádi, P. Hvizdoš, F. Lofaj, J. Dusza, Indentation hardness and fatigue of the constituents of WC-Co composites, Int. J. Refract. Met. Hard Mater. 49 (2015) 178-183.

[18] Y.H. Ren, B. Zhang, Z.X. Zhou, Specific energy in grinding of tungsten carbides of various grain sizes, CIRP Ann. - Manuf. Technol. 58 (2009) 299-302.

[19] J. Heinrichs, M. Olsson, K. Yvell, S. Jacobson, On the deformation mechanisms of cemented carbide in rock drilling-Fundamental studies involving sliding contact against a rock crystal tip, Int. J. Refract. Met. Hard Mater. 77 (2018) 141-151.

[20] Q. Zhang, Q. Zhao, S. To, B. Guo, W. Zhai, Diamond wheel wear mechanism and its impact on the surface generation in parallel diamond grinding of RB-SiC/Si, Diam. Relat. Mater. 74 (2017) 16-23.

[21] G. Zhang, Y. Dai, S. To, X. Wu, Y. Lou, Tool interference at workpiece centre in single-point

diamond turning, Int. J. Mech. Sci. 151 (2019) 1-12.

[22] Q. Zhang, S. To, Q. Zhao, B. Guo, Surface damage mechanism of WC/Co and RB-SiC/Si composites under high spindle speed grinding (HSSG), Mater. Des. 92 (2016) 378-386.

[23] S. Chen, C.F. Cheung, F. Zhang, C. Zhao, Three-dimensional modelling and simulation of vibration marks on surface generation in ultra-precision grinding, Precis. Eng. 53 (2018) 221-235.

[24] C.F. Cheung, W.B. Lee, Characterisation of nanosurface generation in single-point diamond turning, Int. J. Mach. Tools Manuf. 41 (2001) 851-875.

[25] H. Saito, A. Iwabuchi, T. Shimizu, Effects of Co content and WC grain size on wear of WC cemented carbide, Wear 261 (2006) 126-132.

[26] K.P. Mingard, H.G. Jones, M.G. Gee, B. Roebuck, J.W. Nunn, In situ observation of crack growth in a WC-Co hardmetal and characterisation of crack growth morphologies by EBSD, Int. J. Refract. Met. Hard Mater. 36 (2013) 136-142.